PROPER MOTION OF COMPONENTS IN 4C39.25

J.C. GUIRADO
Instituto de Astrofísica de Andalucía, CSIC, 18080 Granada, Spain, and
Jet l'repulsion laboratory, California Institute of Technology, Pasadena, California 91109
Electronic. mail: jcg@fora.jpl.nasa.gov

J.M. MARCAIDE
Departamento de Astronomía, Universitat de València, 46100 Bu rjassot, Spain, and
Harvard-Smithsonian Center for Astrophysics, Cambridge, Massachusetts 02138
Electronic mail: jmm@vlbi.matapl.uv.es

A. ALBERDI
Instituto de Astrofísica de Andalucía, CSIC, 18080 Granada, Spain, and
Laboratorio de Astrofísica Espacial y Física Fundamental, INTA, 28080 Madrid, Spain
Electronic mail: alberdi@laeff.esa.es

1'. ELÓSEGUI, M.]. RATNER, 1.1. SHAPIRO
Harvard-Smithsonian Center for Astrophysics, Cambridge, Massachusetts 02138
Electronic mail: closegui@cfa.harvard.edu, mir@cfa.harvard.edu, shapiro@cfa.harvard.edu

R. KILGER
Satellitenbeobachtu gestation Wettzell, 93444 Koetzting, Germany
Electronic mail: wvax1::vlbi

F. MA NTOVANI , T. VENTURI
Istituto di Radioastronornia, CNR, 40129 Bologna, Italy
Electronic mail: fmantovani@astbo1.bo.cnr.it, tventuri@astbo1.bo.cnr.it

A. RIUS
Centro de Estudios Avanzados, CSIC, Blanes, 17300 Barcelona, Spain, and
Laboratorio de Astrofísica Espacial y Física Fundamental, 1 NTA, 28080 Madrid, Spain
Elect ronic mail: rius@mach.laeff.esa.es

E. Ros
1 Departamento de Astronomic, Universitat de València, 46100 Burjassot, Spain
Electronic mail: ros@vlbi.matapl.uv.es

C. TRIGILIO
Istituto di Radioastronomia, CNR, 96017 Noto, Italy
Electronic mail: trigilio@irant1.ira.noto.cnr.iit

A. It. WHITNEY
NEROC Haystack observatory, Westford, Massachusetts 01886
Electronic mail: arw@wells.haystack.edu

Submitted to: The Astronomical Journal

ABSTRACT

From a series of simultaneous 8.4 and 2.3 GHz VLBI observations of the quasar 4C39.25 phase-referenced to the radio source 0920-1-390, carried out in 1990-1992, we have measured the proper motion of component b in 4C39.25:

$$\mu_\alpha = 90 \pm 35\ \mu\text{as/yr}$$
$$\mu_\delta = 6 \pm 63\ \mu\text{as/yr}$$

where the uncertainties represent standard errors. This proper motion is consistent with earlier interpretations of VLBI hybrid mapping results, which showed an internal motion of this component with respect to other structural components. Our differential astrometry analyses show component b to be the one in motion. Our results thus further constrain models of this quasar.

1. INTRODUCTION

The radio source 4C39.25 (0923+392) is an 18th magnitude quasar with a redshift of 0.699 (Hewitt & Burbidge 1980). It is one of the brightest compact sources on the sky at centimeter wavelengths. The structure of 4C39.25 at the milliarcsecond (mas) angular scale consists of four components, labelled a, b, c, and d, from east to west (see Fig. 1). Since the early VLBI observations of Shaffer *et al.* (1977), components a and c have remained stationary with respect to each other, while component b (first identified by Marcaide *et al.* 1985) has been moving superluminally from near c

towards a (Shaffer *et al.* 1987; Marscher *et al.* 1987; Schalinski *et al.* 1988; Marcaide *et al.* 1989; Marscher *et al.* 1991; Alberdi *et al.* 1993a). These maps show that none of these three components had the inverted or flat spectrum associated with the core of a superluminal source. However, component d, detected via sensitive 22 GHz VLBI observations (Marcaide *et al.* 1990; Alberdi *et al.* 1993a), remains stationary with respect to a and c and possesses an inverted spectral index (Alberdi *et al.* 1993a,b) indicating that it, could be the core of 4C39.25.

Based on these observational facts, Marcaide *et al.* (1989), Marscher *et al.* (1991), and Alberdi *et al.* (1993a) suggested a model for this source which has a relativistic bent jet; the knots a and c are associated with bends of the jet and b with a shock wave travelling along the jet from c towards a. In this model d is considered as the core of the radio source. Since this model is based on the assumption that both a and c are stationary, a much stronger constraint than existing observational evidence for relative stationarity would be evidence for (or against) stationarity with respect to an external reference (Marcaide *et al.* 1990).

In this paper we report the result of a series of VLBI observations of 4C39.25 phase-referenced to the nearby radio source 0920+390 (separated by only 0°.75 on the sky). We assume this source to be stationary; its redshift is unknown. While conventional VLBI mapping provides information only about the relative position between different features of a given radio source, phase-reference observations can provide

precise positional information with respect to an external reference. In our analysis, we used the fringe-phase observable and differential astrometry techniques (Guirado *et al.* 1995 and references therein) to measure the motion of the component b with respect to the radio source 0920+390. Preliminary results of these observations were published earlier by Marcaide & Guirado (1 993).

This work is a part of a broader study (see overview by Marcaide *et al.* 1994) of this '(peculiar') superluminal radio source. The study includes numerical simulations of the relativistic jet (Alberdi *et al.* 1993a; Gómez *et al.* 1994), 43 GHz VLBI observations (Alberdi *et al.* 1993b), and VLBI polarization observations (Marscher *et al.* 1991).

We observed each of our two sources in right circular polarization, in two frequency bands (~8.4 GHz and ~2.3 GHz) simultaneously. 'J'able 1 shows the epochs of observations, the recording mode, and the telescope arrays used in these observations. We interleaved observations of the two sources using a 7 min observing cycle which consisted of 2 min on 4C39.25, 3 min on 0920+ 390, and 1 min slew time for each source change. The data were correlated at the correlator of the Max Planck Institut für Radioastronomie in Bonn. We fringe fitted the data and obtained, for each source scan, the group delay, the phase-delay rate, and the fringe phase (modulo

27r) at the refer-cmcc frequencies 8405 and 2275 MHz for each of the epochs 1990.32 and 1992.18, and 8291 and 2231 MHz for the epoch *1991.22.* We were forced to use a different frequency configuration at the second epoch, compatible with geodetic standards, to avoid wiring changes at some sites. Despite the slight difference in reference frequencies, we will use hereafter the terms 8.4 GHz and 2.3 GHz to identify both maps and observables referred to these frequency bands. The *uv* coverage is very similar in all three experiments (see Fig. 2); the resolution of our array is higher in right ascension than in declination, as can be seen in the corresponding synthesized beams (see Table I). High resolution in right ascension favors the detection of proper motion in 4C39.25, since component b is moving eastwards relative to the others components.

3. MAPS OF THE RADIO SOURCES

We used the program DIFMAP (Shepherd *et al.* 1995), a part of the Caltech VLBI Package (Pearson 1991), to obtain maps of 4C39.25 and 0920+390 at the three epochs in each frequency band. Figs. 3 and 4 show the maps for both sources at 8.4 and 2.3 GHz, respectively. At 8.4 GHz, the structure of 4C39.25 is dominated by the brightest component, b (Alberdi *et al.* 1993a), although this component is partly blended with component a at this frequency. The components c and d are hardly detectable because of the limited dynamic range of our maps and the spectra of the components. At the 2.3 GHz frequency band, 4C39.25 appears point-like and none of the components can be distinguished. Note that, during the two year span of our

observations, the flux density of 4C39.25 at 8.4 GHz increased while its flux density at 2.3 GHz decreased.

The characteristics of the flat-spectrum radio source 092(] -{390 were first catalogued by Ficarra *et al.* (1 985). Its structure is pointlike at both VLA (Vigotti *et al.* 1989; Patnaik *et al.* 1992) and VLBI scales (this paper). The unresolved structure of 0920+390, its proximity to 4C39.25 on the sky, and its flux density, which always exceeded 0.2 Jy at 8.4 GHz, combine to make 0920+390 a good reference source. However, the absence of an optical identification for 0920+ 390 is a concern in the interpretation of our results. A search for an optical identification was first carried out by Vigotti *et al.* (1 989) by scanning the Palomar Observatory Sky Survey (POSS) prints. The negative result of this search implies that the object is fainter than magnitude 20 in red and 21 in blue (POSS magnitude cutoffs). We cannot rule out that 0920+390 corresponds to an object in our vicinity, although the combination of its radio and optical properties makes that possibility seem very unlikely.

4. ASTROMETRIC ANALYSIS

Our astrometric analysis of the data from each observing epoch is similar to that of previous astrometric studies that used phase delay, the most precise VLBI observable (Shapiro *et al.* 1979; Bartel *et al.* 1986; Guirado *et al.* 1995). To correct the phase delays for their inherent 2π ambiguity, we first constructed models of the prop-

agation medium and of the geometry of the array to produce theoretical estimates of our observables. The values of the parameters of these models and their origins are listed in Table 2. Using these models along with estimates of the relative drifts of the station clocks, obtained from a weighted-least-squares analysis of the group-delay and phase-delay rate data with an extensively improved version of the VLBI3 program (Robertson 1975), we generated theoretical phase-delay rates that fit each of the observed phase-delay rates to within 0.1 ps/s (0.5 ps/s) at 8.4 GHz (2.3 GHz), which, considering the duty cycle (7 min), sufficed for predicting the phase behavior between consecutive observations of each source at each frequency band at each epoch. We also corrected for possible remaining "overall ambiguities" (integer number of phase cycles by which the phase delays for one source might be offset from those of the other at each baseline and frequency band during the observations at each epoch) by estimating them via the weighted-least-squares analysis. We then fixed each overall ambiguity to the nearest integer to the weighted-least-squares estimate (for each epoch, baseline, and frequency band, our estimate of the overall ambiguity was closer to an integer number than one sixth of the ambiguity interval).

4.1 Radio Source Structure Correction

We have used the maps in Figs. 3 and 4 to subtract the structure contribution from the total phase delay in each case. To calculate this structure phase, we tried to select as a reference point the feature on the brightness distributions from the

successive epochs of data that we could identify most reliably and accurately. We detail below the way this reference point was selected.

4.1.1 Reference-point selection at 8.4 GHz

To determine proper motion, or to place a stringent bound on it, we should select as the reference point in 4C39.25 the same physical feature of the radio source at all the observing epochs. Were the maximum of the brightness distribution in component b, it would be a useful reference point, since we would be able to monitor or to bound directly its motion. However, at 8.4 GHz we cannot reliably discriminate between components b and a; therefore, we selected as the reference point the maximum of the brightness distribution constructed by convolving the delta components of the CLEAN model with a beam twofold smaller than the synthesized beam. Thus, the reference point location is approximately the brightness centroid of components a and b (see Fig. 5). For 0920+390, at each epoch, we selected the maximum of the brightness distribution, constructed by convolving the delta components of the CLEAN model with the synthesized beam; this position corresponds to the unresolved component which is presumably the core of this radio source. The sensitivity of our result to these choices of reference points is discussed in Section 4.5.

4.1.2 Reference-point selection at 2.3 GHz

We combined the 8.4 GHz and 2.3 GHz data, as if the source positions were identical at the two frequencies, in order to estimate and largely remove the plasma contribution to the phase delay. Therefore, for each observing epoch, the phase delays at both frequencies should be referred to the same point on the radio source structure; thus, we tried to determine which point in the 2.3 GHz radio structure corresponds to the reference point selected at 8.4 GHz.

Since component b of 4C39.25 is self-absorbed at 2.3 GHz (Marscher *et al.* 1991; Fig. 6), we may expect a shift of the peak of brightness at 2.3 GHz with respect to that at 8.4 GHz (Marcaidc & Shapiro 1984). Therefore, instead of referring the phase delays to this component, we used the optically thin component c of the jet of 4C39.25 to "register" the 8.4 and 2.3 GHz maps. This method of registration of maps at different frequencies by registration of an optically thin feature has been used previously for other sources to measure proper motions (Bartel *et al.* 1986) and to obtain spectral information (Chariot 1993). The registration for 4C39.25 is shown in Fig. 7; in particular, the maps used for this registration were obtained from a ten station 8.4/2.3 GHz VLBI experiment carried out at epoch 1990.55 (see Rioja 1993 for details) and of higher quality than those presented in Figs. 3 and 4. Both maps of Fig. 7 are centered on their respective peak of brightness; component c appears shout, 2 and 2.5 mas west for the 8.4 and 2.3 GHz maps, respectively. Therefore,

wc registered the maps by shifting the 2.3 GHz map 0.5 mas eastwards relative to the 8.4 GHz map. Since component c cannot be distinguished in the 8.4 GHz maps at the other epochs, wc could not usc the same process at these epochs to obtain reliable registrations. However, the morphological similarity of all the 2.3 GHz maps indicates that any change in this registration between 1990.55 and the earlier and later epochs of our observations is unlikely to be large compared to 0.5 mas. Given the relative insensitivity of our plasma corrections to the registration of the maps for the two frequency bands, our usc of the 0.5 mas eastward displacement for all the 2.3 GHz maps is a safe choice. The sensitivity of our astrometric results to this registration is discussed in Section 4.5.

Any shift between the peaks of brightness at 8.4 and 2.3 GHz for the radio source 0920-t 390 is not detectable in our maps because the source is pointlike at the resolutions achieved. On the other hand, the change from epoch to epoch of the shift, if any, in this source is expected to be much smaller than that in 4C39.25 since 0920+390 has not shown any detectable change with time either in structure or in flux density. The constancy of this source supports that its structure dots not contribute to any apparent relative motion of the two sources.

Wc estimated the structure phases with respect to the selected reference points from the hybrid maps by using the Caltech program PHASE (Readhead & Wilkinson 1978). At each epoch and frequency band, the corresponding structure-]lhasc delays

were subtracted from the total phase delays. These adjustments were each less than 5 ps.

4.2 Propagation Medium Correction

For the phase delay, we estimated the plasma contribution through its ν^{-2} dependence. For each epoch, we combined the simultaneously measured phase delays at 8.4 and 2.3 GHz as follows:

$$\tau_{free} = \frac{R(\tau_x - \tau_x^{str}) - (\tau_s - \tau_s^{str})}{R - 1} \quad (1)$$

where τ_{free} is the plasma-free, or "dual-frequency" delay, τ_x and τ_s are the observed delays at 8.4 and 2.3 GHz, respectively; τ_x^{str} and τ_s^{str} are the corresponding structure delays; and R is the square of the ratio between the center frequencies of the two bands $(8.4/2.3)^2 \sim 13$. Although no apparent incorrect connections of the phase delay are visible in our data, any such misconnection at either of the frequency bands would affect the estimate of the dual-frequency phase delay according to the above expression; for example, one 2n-equivalent connection error at 8.4 GHz (2.3 GHz) is equivalent to a 128.6 (35.6) ps error in the dual-frequency delay.

Alternatively, an independent estimate of the plasma contribution can be obtained from the group delays by using Eq. 1. However the accuracy of this estimate is limited by the standard deviation of our group delays, ~ 1 ns, and hence, the corresponding

differential position is too coarse, ~ 10 mas standard error in each coordinate, to be of use in achieving our goal to measure the proper motion of b in 4C39.25.

We used meteorological data obtained at each site and the model of Saastamoinen (1 973) to calculate a priori average values for the tropospheric delay at local zenith due to the "dry" and "wet" components of the troposphere. We used the CfA2.2 mapping function (Davis *et al.* 1985) to determine the tropospheric delay at non-zenith elevations. Since our lowest antenna elevation was 15° and since the two sources observed are so close on the sky, use of other simpler mapping functions, such as Chao's (1 974), produced no significant differences in our astrometric results (less than 10 μas in the estimates of the relative position of the sources).

4.3 Differenced Observable

We formed differenced phase-delays by subtracting the phase delay of each observation of 0920+390 from the previous observation of 4C39.25, typically 4 min earlier; this scheme avoids the effects of the 10 min gaps in the data due to the MkIII tape changes. An alternative pairing scheme, forming differenced observables by subtracting the phase delay of each observation of 4C39.25 from the previous one of 0920+-390, gave similar results when we discarded those observation pairs whose time difference is larger than 10 min due to tape-changc gaps. (liven the small angular separation between these wo sources (0°.75), imprecisely modelled effects, such as for the tropo-

sphere, are to a great extent cancelled in the differenced observables.

4.4 Weighted-least-squares Analysis

Our weighted-least-squares result for the position of 4C39.25 with respect to that of 0920+390 for each observing epoch depends primarily on the differenced phase-delays. The undifferenced phase-delays for 4C39.25 were also included in the analysis to allow us to estimate the relative behavior of the site clocks. The standard deviations of the differenced phase-delays and the 4C39.25 phase-delays were scaled separately so that, for each type, the weighted-l ncan-square of the postfit residuals was unity. Parameters for tropospheric zenith delays, site coordinates, 4C39.25 coordinates, Earth pole coordinates, and UT1-UTC were included in the analysis, with their adjustments constrained by their a priori values and corresponding standard deviations, given in 'J'able 2, through the usc of an a priori covariancc matrix; software limitations prevented us from also solving for adjustments to the Earth's nutation. Wc also estimated in our analysis, without any a priori constraint (since we did not have any previous or useful knowledge about them), the right ascension and declination of 0920+390, and, for each site excepting Madrid, the coefficients of a polynomial of degree three that was used to represent the behavior of that site's clock relative to Madrid's. The position of 4C39.25 with respect to 0920+390 obtained from the analysis of the data from each of the three epochs is shown in '1'able 3. We refer to these positions as "dual-frequency" positions, since the phase delays

used in our analyses are a linear combination of the phase delays at both frequency bands according to Eq. 1.

4.5 Error Analysis

Contributions to the standard errors Of $\Delta\alpha$ and $\Delta\delta$ ($\Delta\alpha \equiv \alpha_{4C39.25} - \alpha_{0920+390}$ and $\Delta\delta \equiv \delta_{4C39.25} - \delta_{0920+390}$) not included in our weighted-least-squares analysis arc those associated with reference-point misidentifications on the 8.4 GHz maps, misregistration of 8.4 and 2.3 GHz maps, and Earth's nutation.

To estimate the standard errors, σ_{peak}, associated with the reference point identification on the 8.4 GHz maps, wc first estimated the standard error in the location of the brightness peak of each source duc to the finit c signal- to-noise ratio, σ_{snr}, using the expression (Thompson, Moran, and Swenson 1986; Fomalont 1989):

$$\sigma_{snr} = \frac{B_p}{2\pi \mathrm{SNR}_{peak}} \qquad (2)$$

where B_p is the width of the main lobe of our synthesized beam, and SNR_{peak} is the signal-to-noise ratio of the map feature used as a reference ($\sim$100 for 4C39.25 and $\sim$50 for 0920+ 390). The estimates of σ_{snr} (the root-sum-square, or rss, of the values for each source) arc shown in '1'able 4 for each coordinate and epoch.

Second, for each 8.4 GHz map, we calculated the difference between the location of the maximum of the brightness distribution (see Section 4.1.1) and the location of the centroid of the significant CLEAN-components (those with flux density larger than 25% of the component with maximum flux density, and located within the main lobe of the synthesized beam when the latter is centered on the position of the largest delta-component). The differences between the locations on the map obtained by these two methods, $\sigma_{M-\delta}$, are, in general, larger than σ_{snr}, due to either errors in the maps and/or the complexity of the brightest feature of the source. To take into account these differences, we take σ_{peak} to be the rss of the corresponding values of $\sigma_{M-\delta}$ and σ_{snr} (see Table 4). Note that, since we scale the 8.4 GHz data by the factor $R/(R-1)$ (about 1.08; see Eq. 1) in calculating the plasma-free delay, the standard errors of $\Delta\alpha$ and $\Delta\delta$ due to the uncertainty of the 8.4 GHz reference point increases by a similar factor. See Table 5.

We also estimated the contribution of the errors in the registration of the maps for the two frequency bands to the standard error of the determination of the separation between the two sources. In Section 4.1.2 we deduced that the 1990.552.3 GHz map of 4C39.25 should be shifted 0.5 mas eastwards to register properly with the corresponding 8.4 GHz map; to estimate the standard error of this registration we calculated σ_{peak} of component c in the 1990.55 maps at both frequencies (we followed a similar procedure to that previously described for the determination of the standard error associated with the reference point identification: for each map we took σ_{peak} to

be the rss of the values for σ_{snr} and $\sigma_{M-\delta}$). Finally, the rss of the σ_{peak} values for both maps yields a standard error in map registration of 300 pas. Note, however, that our final results do not depend critically on this estimate because we scale the 2.3 GHz data by the factor $(R - 1)^{-1}$ (about 0.08; see Eq. 1) in calculating the plasma-free delay. The 300 μas estimated standard error undergoes a similar scaling, so that the standard error of $\Delta\alpha$ and $\Delta\delta$ due to the uncertainty in the registration of the maps at the two frequency bands is about 24 pas.

In addition, we estimated the sensitivity of our result to errors in our knowledge of the Earth's nutation (see Section 4.4). To estimate the contribution of such errors to the standard error of the estimates of $\Delta\alpha$ and $\Delta\delta$, we altered the nutation in longitude and obliquity, one at a time, by one standard deviation (values given in footnote to Table 2), and in each case repeated the weighted-least-squares analysis to obtain the shift of the relative position of the two sources. The resulting displacements are shown in Table 5 and regarded as standard errors. Note that this technique fails to account for the correlations between the estimate of each of these parameters with the other as well as with all of the other parameters; however, in view of the small values of these changes and of the expected differences in "signatures" between all of these parameters, this neglect of correlations should have no significant effect on our estimate of the overall standard errors.

Thus, for each epoch, we estimated the overall standard errors of the position of

4C39.25 with respect to the position of 0920+390 as the rss of the standard deviations of all the contributions discussed above (see 'Table 5).

5. COMPARATION WITH OTHER POSITION ESTIMATES

Comparisons of our relative position for 4C39.25 and 0920+390 with other VLBI estimates are possible. Both sources are included in the NAVNET (Navy VLBI Network) program carried out by the US Naval Observatory (USNO). We calculated the arclength between the two sources (this quantity is invariant to rotation and, therefore, independent of the reference system where the source coordinates are defined) from our weighted mean relative position (see 'Table 3) and from the positions of the most recent USNO solution available (N9504; M. Eubanks private communication). These values are:

arc (4C39.25,0920+390; this paper):	46′ 13!'3031 3	±0.″00006
arc (4C39.25,0920+390; USNO):	46′ 13!'3029	±0.″0003

The two arclengths agree to within the rss of their standard deviations, even though some difference between these values might have been expected: the lack of any correction for source structure in the USNO analysis prevent precise comparisons between the two sets of position results. From the comparison between the location of the maximum and the centroid of our brightness distributions of 4C39.25 and 0920+390, we estimated that source-structure effects could shift the relative position by about 300 μas (due to the structure of 4C39.25).

6. RESULTS

The right ascensions and declinations of 4C39.25 relative to 0920+390 with their overall standard errors and correlations are represented in Fig. 8, which shows a net increase with time of the eastward separation of the component b of 4C39.25 from 0920-{-390. To quantify this result we used the relative coordinates and their associated standard errors in two separate weighted least-squares analyses to estimate the proper motion in each coordinate (see Fig. 9):

bution of the radio sources, than of proper motion of the center of mass of either source. Since 0920+390 has not shown significant changes in strut.turc during the interval spanned by our observations, wc infer that the proper motion is due to internal changes in the radio structure of 4C39.25. More specifically, this proper motion is consistent with a motion of the component b along the jet of 4C39.25 from c towards a. Assuming that 0920+390 has a negligible proper motion (see Section 3 for relevant discussion), wc obtain the corresponding velocity components for the reference point in 4C39.25:

$v_\alpha = 1.97 \pm 0.77$ c
$v_\delta = 0.13 \pm 1.38$ c

for H_0=100 $kms^{-1}Mpc^{-1}$ and q_0=0.5.

7. CONCI,US1ONS

Wc have measured the eastward proper motion of component b in 4C39.25 with respect to the unresolved source 0920+-390. This pi opcr motion is compatible with the results inferred from the hybrid mapping of 4 C39.25 (Marcaide *et al. 1989;* Marscher *et al.* 1991; Alberdi *et al.* 1993a) and together with them it shows that component b is moving from west to cast, while the separation of components a and c remains fixed.

Measurements of the motion of component b (Alberdi *et al.* 1 993a) between 1987 and 1989, based on hybrid mapping, yielded 110.EIO μas/yr with respect to compo-

nents a and c. Using more recent observations made from 1991 to 1993, Alberdi *et al.* (1995) employed the same hybrid mapping techniques and obtained a corresponding proper motion of b relative to a and c of 60 ± 30 μas/yr. Note that, since no astrometric analysis was necessary in the latter measurements, their standard deviations are only due to the misidentification of the components of 4(139.25 on high quality maps and, consequently, they are smaller than the standard deviation of our proper motion measurement. However, none of these map measurements determines, for example, whether a and c are stationary components and b a travelling one or vice versa. By comparison, our proper motion measurement provide the following results: component b has a proper motion in right ascension of 90 ± 35 μas/yr relative to an external reference, 0920+390. This value lies between those previously obtained from hybrid maps, as would be expected from a monotonic deceleration of the proper motion of component b. in addition, the consistency of our measurement with the hybrid mapping results, and the stationarity of components a and c relative to each other (to within 30 μas; Alberdi *et al.* 1995) implies that a and c are stationary with respect to the external reference, at least at the level of tile combination] of the uncertainties of both measurements.

With this determination of the proper motion of component b of 4C39.25 we have demonstrated the validity of an essential aspect of the phenomenological and numerical model for 4C39.25 proposed by Marcaide *et al.* (1989), Marscher *et al.* (1991), and Alberdi *et al.* (1993a). The moving character of component b is an argument in

favor of its interpretation as a shock wave.

Additional phase-refcrcmccd observations made during the period 1989-1993 simultaneously at 8.4 and 2.3 GHz are currently being processed. These observations are much more sensitive (due to the large array employed) and should allow us to obtain *(i)* an improvement of the measurement of proper motion in 4C39.25, and *(ii)* more useful bounds on the station arity of components a and c. The latter is especially interesting for component a, since component b is moving towards a and would reach the latter's sky position bet wccn 1995 and 2001 (A. Alberdi, private communication), these components should not be distinguishable at centimeter wavelengths. We may then check to determine whether, for example, component a suffers a significant change in its position after the "collision", as predicted by the standing shock theory of Daly & Marscher (I 988), or whether it remains stationary, as predicted by the twisted jet mode] (see Section 1). Complementary phase--refcrcnccd observations made in 1991 at 22 G] Iz arc also being analyzed; at this radio frequency, components a, b, and c are distinguish able, and even d is detectable, so still more accurate bounds on the mot ion of each component should be obtainable.

There are other radio sources that seem to have components travelling between two apparently stationary ones and hence could also be interesting targets of study for differential VLBI astrometry. These sources include 0711 + 356 (Conway *et al.* 1 990), 0735+178 (Bååth *et al.* 1991), 1803-! 784 (Witzel *et al.* 1988), and 3C395 (Lara *et al.*

1994). Though the morphology and internal kinematics of these sources may be similar to those of 4(239.25, they might be produced by different physical mechanisms; therefore, detailed monitoring of the motion (or lack of it) of the components in these sources would help us to understand the nature of the physical processes involved.

ACKNOWLEDGMENTS. We thank the staffs of the various observatories for their contribution to the observations, aud the staff at the MPIfR correlator for their efforts during the correlation. J.C.G. acknowledges the receipt of an }1'1 grant from the Junta de Andalucía for this research. A portion of this work was performed while J.C. G. held a National Research Council-J PL Research Associateship. This work has been partially supported by the Spanish DGICYT grant PB89-0009 and the U.S. National Science Foundation Grant AST-9303527. J]'], is operated by Caltech, under contract with NASA.

REFERENCES

Alberdi, A., Marcaide, J. M., Marscher, A.] '., Zhang, Y.F., Elósegui, P., Gómez, J.I,., and Shaffer, D.B. 1993a, ApJ, 402, 160

Alberdi, A., Krichbaum, '1'.1'., Marcaide, J. M., Witzel, A., Graham, D.A., Inoue, M., Morimoto, M., Booth, R. S., Rönnäng, B.O., Colomer, 1'., Rogers, A. E.It., Zensus, J. A., Readhead, A. C. S., Lawrence, C. R., Vermeulen, R., Bartel, N., Shapiro, 1.1., and Burke, B.F. 1993b, A&A, 271, 93

Alberdi, A., Krichbaum, '1'.1'., Marcaidc, J. M., Witzel, A., Standke, K., Graham, 1). A., Schalinski, C. J., Grewing, M., Greve, A., Booth, 1{. S., Bååth, L.B., Colomer, F., Rogers, A.E.E., Doeleman, S., and Zensus, J.A. 1995, A&A, in preparation

Bååth, L.B., Zhang, F.J., and Chu, 11. S. 1991, A&A, 250, 50

Bartel, N., Herring, '1'. A., Ratner, M. I., Shapiro, 1.1., and Corey, B.E. 1986, Nature, 319, 733

Chao, C.C. 1974, JPL/NASA Tech. Rep., No. 32-1587, 61

Charlot, 1'. 1993. In: Sub Arcsecond Radiastronomy, Davis, R., and Booth, R.S. (eds.), Cambridge: Cambridge University Press, p. 218

Conway, J.E., Unwin, S. C., Pearson, T. J., Readhead, A. C. S., and Xu, W. 1990. In: Proc. 1 Dwingeloo Workshop on Compact- Steep Spectrum and GHz-Peaked Spectrum Radio Sources, Fanti, C., Fanti, R., O'Dea, C.] '., and Schilizzi, R.T.

(eds.), Bologna: Istituto di Radioastronomia, 1,.157

Daly, I{.. A., and Marscher, A.]'. 1988, AJ, 334, 539

Davis, J.],., Herring, 'l'. A., Shapiro, 1.1., Rogers, A.E.E., and Elgered, G. 1985, Radio Sci., 20, 1593

Feissel, M., and Essaïfi, N. (eds.) 1993, IERS Annual Report for 1992, Paris: Observatoire du Paris

Ficarra, A., Grueff, G., and Tomassetti, G. 1985, A&AS, 59, 255

Fleagle, R. G., and Businger, J.A. 1980, An Introduction to Atmospheric Physics, Orlando: Academic Press

Fomalont, E. 1989. In: Synthesis imaging in Radio Astronomy, Perley, R.A., Schwab, F.R., and Bridle, A.H. (eds.), ASP Conference Sm-its, Vol. 6, p. 213

Gómez, J.],., Alberdi, A., and Marcaide, J.M. 1994, A&A, 284, 51

Guirado, J. C., Marcaide, J. M., Elósegui, 1'., Ratner, M.]., Shapiro, 1.1., Eckart, A., Quirrenbach, A., Schalinski, C. J., and Witzel, A. 1995, A&A, 293,613

Hewitt, A., and Burbidge, G. 1980, ApJS, 43, 57

Lara, 1,., Alberdi, A., Marcaide, J. M., and Muxlow, '1'. W. B. 1994 A&A, 285, 393

Lieske, J.]]., Lederle, 'l'., and Fricke, W. 1977, A&A, 58, 1

Marcaide, J. M., and Shapiro, 1.1.1984, ApJ, 276, 56

Marcaide, J. M., Bartel, N., Gorenstein, M. V., Shapiro, 1.1., Corey, B.E., Rogers, A.E.E., Webber, J. C., Clark, '1'. A, Romney, J.])., and Preston, R.A. 1985, Nature, 314, 424

Marcaide, J. M., Alberdi, A., Elósegui, 1'., Schalinski, C. J., Jackson, N., and Witzel,

A. 1989, A&A, 211, 1,23

Marcaide, J. M., Alberdi, A., Elósegui, I'., Marscher, A.I'., Zhang, Y. F., Shaffer, D.B., Schalinski, C. J., Witzel, A., Jackson, N., and Sandell, G. 1990. In: Parsec-scale Radio Jets, Z ensus, J. A., and Pearson, T.J. (eds.), Cambridge: Cambridge University Press, p. 236

Marcaide, J. M., and Guirado, J.C. 1993. In: Very nigh Angular Resolution Imaging, IAU Symposium 158, Robertson, J.G, and Tango, W.J. (eds.), Dordrecht: Kluwer Academic Publishers, p. 445

Marcaide, J. M., Alberdi, A., Gómez, J.],., Guirado, J. C., Marscher, A.] '., and Zhang, Y.F. 1994. In: Compact Extragalactic Radio Sources, Zensus, J. A., and Kellermann, K.]. (eds.), Socorro: National Radio Astronomy observatory, p. 141

Marscher, A.]'. 1987. In: Superluminal Radio Sources, Zensus, J. A., and Pearson, T.J. (eds.), Cambridge: Cambridge University Press, p. 280

Marscher, A.] '., Zhang, Y.F., Shaffer, D.B., Aller, H.D., and Aller, M.F. 1991, ApJ, 371, 491

McCarthy, D.D. (cd.) 1992, IERS Technical Not c 13: IERS Standards, Paris: Observatoire du Paris

Patnaik, A.R., Browne, I. W. A., Wilkinson, P.N., and Wrobel, J.M. 1992, MNRAS, 254, 655

Pearson, T.J. 1991, BAAS, 23, 991

Readhead, A. C. S., and Wilkinson, P.N. 1978, ApJ, 223, 25

Rioja, M.J. 1993, Ph.D. thesis, Universidad dc Granada

Robertson, D.S. 1975, Ph.D. thesis, Massachusetts Institute of Technology

Rogers, A.E.E., Cappallo, R. J., Hinteregger, H.F., Levine, J. I., Nesman, E'., Webber, J. C., Whitney, A.R., Clark, T. A., Ma, C., Ryan, J., Corey, B.E., Counselman, C. C., Herring, T. A., Shapiro, 1.1., Knight, C. A., Shaffer, D.B., Vandenberg, N.R., Lacasse, R., Mauzy, R., Rayhrer, B., Schupler, B. R., and Pigg, J.C. 1983, Science, 219, 51

Rönnäng, 11.0.1989. In: Very Long Baseline Interferometry, NATO ASI Series, Felli, M., and Spencer, R.E. (eds.), Dordrecht: Kluwer Academic Publishers, p. 305

Saastamoinen, J. 1973, Bull. Géodésique, 105, 279

Schalinski, C. J., Alberdi, A., Elósegui, T., and Marcaide, J.M. 1988. In: The Impact of VLBI on Astrophysics and Geophysics, IAU Symposium 129, Reid, M. J., and Moran, J.M. (eds.), Dordrecht: Kluwer Academic Publishers, p. 39

Shaffer, D.B., Kellerman, K.J., Purcell, G.H., Pauliny-Toth, 1.1.1 <., Preuss, E., Witzel, A., Graham, D., Schilizzi, R.T., Cohen, M.H., Moffet, A.T., Romney, J.D., and Niell, A.E. 1977, ApJ, 218, 353

Shaffer, D.B., Marscher, A.P., Marcaidc, J. M., and Romney, J.D. 1987, ApJ, 314, 1.1

Shapiro, 1.1., Wittels, J. J., Counselman 111, C. C., Robertson, 1). S., Whitney, A.R., Hinteregger, H.F., Knight, C. A., Rogers, A.E.E., Clark, T. A., Hutton, L. A., and Niell, A.E. 1979, A,J, 84, 1459

Shepherd, M. C., Pearson, T. J., and Taylor, G.B. 1995, BAAS, 26, 987

Thompson, A.R., Moran, J. M., and Swenson, G.W. 1986, Interferometry and Synthesis in Radio Astronomy, New York: Wiley

Vigotti, M., Grueff, G., Perley, R., Clark, B. G., and Bridle, A. 11.1989, AJ, 98, 419

Witzel, A., Schalinski, C. J., Johnston, K. J., Biermann, 1'.1,., Krichbaum, '1'.1'., Hummel, C. A., and Eckart, A. 1988, A&A, 206, 245

FIGURE CAPTIONS

Figure 1. Map of the quasar 4C39.25 at 22 GHz in 1988 (Alberdi *et al.* 1993a). Four components, labelled a, b, c, and d, are distinguished. Contours are -0.5, 0.5, 1, 2, 5, 10, 30, 50, 70, and 90% of the peak of brightness, 1.58 Jy/beam. Dashed lines correspond to negative contours. The size of the restoring beam, shown at the bottom left corner, is 0.50 x 0.24 mas with a major axis position angle of -12".

Figure 2. *uv*-coverage corresponding to the 8.4 GHz observations shown in Table 1 for the source 4C39.25. The *uv*-coverage for 0920+390 is very similar because the two sources are very close together on the sky.

Figure 3. Hybrid maps of 4C39.25 and 0920+390 at 8.4 GHz. For the 4C39.25 maps, contours are -1, 1, 2, 4, 6, 10, 15, 22, 30, 42, 60, 80, 95% of the peak of brightness of each map, which, chronologically ordered, are: 4.76, 6.15 and 6.31 Jy/beam. The corresponding total map flux densities are 7.4 ± 0.7, 9.6 ± 0.7, and 9.8 ± 0.7 Jy. For the 0920+390 maps, contours are -2, 2, 4, 6, 10, 15, 22, 30, 42, 60, 80, 95% of the peak of brightness of each map, which, chronological] y ordered, are: 0.40, 0.25 and 0.30 Jy/beam]. The corresponding total map flux densities are 0.45 ± 0.04, 0.32 ± 0.03, and $0.30+0.03$ Jy. The uncertainties quoted are peak-to-peak values from a set of

trial maps made with an overall 10% calibration error (the latter was estimated by comparison between the correlated flux densities of calibrator sources, included in our observing schedules, corresponding to different baselines). Dashed lines correspond to negative contours. The restoring beam (see Table 1 for the corresponding sizes) is shown at the bottom left corner of each map.

Figure 4. Hybrid maps of 4C39.25 and 0920-I 390 at 2.3 GHz. For the 4C39.25 maps, contours are -1, 1, 2, 4, 6, 10, 15, 22, 30, 42, 60, 80, 95% of the peak of brightness of each map, which, chronologically ordered, are: 3.02, 2.60, and 2.44 Jy/beam. The corresponding total map flux densities are 3.6 ± 0.4, 3.4 ± 0.4, and 3.0 ± 0.3 Jy. For the 0920+390 maps, contours are -2, 2, 4, 6, 10, 15, 22, 30, 42, 60, 80, 95% of the peak of brightness of each map, which, chronologically ordered, are: 0.21, 0.20, and 0.22 Jy/beam. The corresponding total map flux densities are 0.21 ± 0.02, 0.24 ± 0.02, and 0.27 ± 0.02 Jy. See caption of Fig. 3 for meaning of quoted uncertainties. Dashed lines correspond to negative contours. The restoring beam (see Table 1 for the corresponding sizes) is shown at the bottom left corner of each map.

Figure 5. Flux-density profiles of 4C39.25 at 8.4 GHz for a position angle of 90°. For each epoch, we show the profiles constructed by using the synthesized beams whose dimensions are shown in Table 1 (thin line) and, superimposed, the profiles constructed by using a restoring beam (thick line) whose dimensions are twofold smaller than those of the synthesized beam. The peak of brightness corresponds to

the maximum of the over-resolved profiles. The components a and b can be distinguished in the first, epoch, but appear partially and totally blended in the second and third epoch, respectively. Flux-density units are arbitrary. See Section 4.1.1.

Figure 6. Total flux density data of 4C39.25 as measured at the Effelsberg telescope (100m, Bonn, Germany) in 1992. The spectrum is dominated by the flux density of component b. Since the source is self-absorbed at 2.3 GHz we may expect a shift of the peak of brightness of the maps between 8.4 and 2.3 GHz. See Section 4.1.2.

Figure 7. We used high-quality 8.4 and 2.3 GHz maps of 4C39.25 at epoch 1990.55 (Rioja 1993) to find their proper registration at 8.4 GHz and 2.3 GHz. We obtained this alignment by superimposing the optically thin regions, component c in this case. Contours are -1, 1, 2, 4, 6, 10, 15, 22, 30, 42, 60, 80, 95% of the peak of brightness of each map, 4.23 and 2.08 Jy/beam, respectively. Total map flux densities are 8.1 $\pm$0.7 and 4.0$\pm$0.4. See caption of Fig. 3 for meaning of quoted uncertainties. Dashed lines correspond to negative contours. The sizes of the restoring beams, shown at the bottom left corners, are 1.21 x 0.62 mas with a major axis position angle of -18° for the 8.4 GHz map and 2.15 x 0.90 mas with a major axis position angle of -18° for the 2.3 GHz map (note that the latter map is over-resolved by a factor two with respect to the dimensions of the corresponding main lobe of the synthesized beam of the array).

Figure 8. Proper motion of component b in 4C39.25 with respect to 0920+390. The positions of Table 3 and their standard deviations (Table 5) are represented; for each epoch, the probability that the relative position is inside the ellipse is 40%. The results indicate proper motion in right ascension.

Figure 9. Proper motion of component b in 4C39.25 with respect to 0920-F390. Values of proper motion in 4C39.25 are shown for three epochs. The straight lines shown represent the results of weighted-least-squares fits to the data for each coordinate separately.

TABLE 1. Observations of 4C39.25 phase-referenced to 0920+390[1]

Epoch	Antennas[2]	Frequencies (GHz)	Synthesized beam[3]
28 April 90 (1990.32)	E, L, M, V	8.4	2.23 x 0.58, 7.8°
		2.3	8.25 x 2.15, 7.8°
21 March 91 (1991.22)	E, 1, L, M, V	8.3	1.40 x 0.62, 3.3°
		2.2	5.22 x 2.30, 3.3°
5 March 92 (1992.18)	E, 1, M	8.4	1.50 x 0.54, 5.7"
		2.3	5.54 x 2.00, 5.7°

[1] We used the MarkII] system in mode B (Rogers *et al.* 1983) to record at two frequencies simultaneously: four 4 MHz adjacent channels centered from 8404.99 to 8416.99 MHz (from 8290.99 to 8302.99 MHz in 1991.22) and three 4 MHz adjacent channels centered from 2274.99 to 2282.99 MHz (from 2230.99 to 2238.99 MHz in 1991.22).

[2] The symbols correspond to the following antennas (with diameter and location given in parentheses): E, Westford (18m, Massachusetts); 1, Noto, (32m, Italy); L, Medicina (32m, Italy); M, DSS63 (70m, Spain); V, Wettzell (18m, Germany).

[3] Sizes of the axes (milliarcseconds) and position angle (degrees, from north to east) of the ellipse corresponding to the contour which is at 50% of the maximum of the synthesized beam.

TABLE 2. Parameters values of the theoretical model

J2000.0 source **coordinates**[1]

4C39.25 (0923+392) $\alpha = 9^h27^m3\overset{s}{.}013902$ $\delta = 39°2'20\overset{''}{.}85231$

Antenna site **coordinates**[1,2]

Antennas	Right-handed cartesian coordinates at 1988.0 (m)			Velocities (m/yr)			Axis offsets[3] (m)
	x	Y	Z	V_X	V_Y	V_Z	
E	1492206.755	-4458130.499	4296015.503	-.0139	-.0040	.0055	0.318
L	4461370.173	919596.665	4449559.103	-.0184	.0189	.0102	1.83
M	4849092.680	-360180.692	4115109.057	-.0072	.0203	.0147	0.0
l	4934563.293	1321201.116	3806484.358	-.0211	.0160	.0152	1.83
v	4075540.048	931735.120	4801629.280	-.0169	.0161	.0092	0.0

Precession Constant (J2000.0)[4]

P=5028.″989/tropical century

Nutation

Predictions of IAU 1980 Nutation Series + IERS daily corrections[1]

UT1 and Polar Motion

Daily values from IERS[1]

Earth Tides

Radial Love number, h = 0.60967

Horizontal Love number, l = 0.085

Tidal lag angle, $\theta = 0°.0$

Propagation medium parameters

Tropospheric zenith delay[5] (ns)

	1990.32		1991.22		1992.18	
	Dry	Wet	Dry	Wet	Dry	Wet
E	7.6	0.3	7.6	0.1	7.7	0.1
L	7.7	0.2	7.7	0.2	-	-
M	7.1	0.3	7.1	0.3	7.1	0.1
l	-	-	7.7	0.3	7.7	0.1
V	7.2	0.2	7.1	0.2	-	-

[1] Data were taken from the International Earth Rotation Service (IERS) 1992 Annual Report (see, also, IERS Technical Note 3 (1989) for tbc standards used in the annual reports). To be conservative, we increased twofold the standard deviations of the IERS parameter estimates that wc used in our analysis. These increased values arc: 4C39.25 coordinates, 0.04 ms in α and 0.5 mas in δ; site positions, 2 cm in each coordinate; nutat ion corrections to the IAU 1980 theory, 1 mas for nutat ion in longitude and 0.4 mas for nutation in obliquity; UT1-UTC, 0.04 ms; each pole coordinate, 1 mas. The daily values for UT1 and polar motion were interpolated to the epochs of observation.

[2] The site positions at the three epochs were calculated by linear extrapolation (using the constant velocities of the coordinates) of the positions at 1988.0.

[3] All the antennas are altitude-azimuth.

[4] From Lieske *et al.* (1977).

[5] The calculation of the "dry" and "wet" tropospheric zenith delays arc described in Section 4.2; their estimated standard errors are 0.07 ns (Fleagle & Bussinger 1980; Davis *et al.* 19S5) and 0.17 rrs (Davis *et al.* 19S5; Rönnäng 1989) for dry and wet components, respectively.

TABLE 3. Dual-frequency estimates of the coordinates of the position of component b of 4C39.25 relative to 0920-390 in J2000.0 system for the three observing epochs[1]

Epoch	$\Delta\alpha$ - 3^{m}48^s.5609770[2] (μas)	$\Delta\delta$ + 12°40''.9418222 (μas)
1990.32	-92 ± 25	-27 ± 84
1991.22	-11 ± 24	20 ± 72
1992.18	76 ± 17	-4 ± 48

[1]The uncertainties shown are the standard errors scaled so that the χ^2 per degree of freedom of the difference observables is unity. See section 4.4.

[2]The reference relative position is the weighted mean of the relative positions from the three epochs.

TABLE 4. Contributions, $\delta\Delta\alpha$ and $\delta\Delta\delta$, of the errors in the reference-point location on the 8.4 GHz maps to the standard errors of the estimates of $\Delta\alpha$ and $\Delta\delta$[1]

	Epoch					
	1990.32		1991.22		1992.18	
	$\delta\Delta\alpha$ (μas)	$\delta\Delta\delta$ (pas)	$\delta\Delta\alpha$ (μas)	$\delta\Delta\delta$ (μas)	$\delta\Delta\alpha$ (μas)	$\delta\Delta\delta$ (μas)
σ_{snr}[2]	4	18	4	10	4	11
$\sigma_{M-\delta}$[3]	38	42	13	8	26	35
σ_{peak}[4]	38	46	14	13	26	37

[1] All the values are the root-sum-square of the individual values for each source.

[2] Standard error in locating the reference point due to the finite signal-to-noise ratio. See text.

[3] Differences in the location of the brightness point between the maximum of the brightness distribution (see Section 4.1.1) and the centroid of the significant delta-components. See text.

[4] Result of addition in quadrature of the values of the two entries above.

TABLE 5. Contributions, $\delta\Delta\alpha$ and $\delta\Delta\delta$, to the standard errors of the dual-frequency estimates of the sky coordinates of 4 C39.25 with respect to those of 0920+390 obtained from the sensitivity study

Effect/Parameter	Epoch					
	1990.32		1991.22		1992.18	
	$\delta\Delta\alpha$ (μas)	$\delta\Delta\delta$ (pas)	$\delta\Delta\alpha$ (μas)	$\delta\Delta\delta$ (μas)	$\delta\Delta\alpha$ (μas)	$\delta\Delta\delta$ (μas)
8.4 GHz reference point identification[1]	41	50	15	14	28	40
8.4/2.3 GHz map registration	24	24	24	24	24	24
Earth's nutation[3]	1	2	1	3	1	2
Statistical standard error[4]	25	84	24	72	17	48
Root-sum-square of the above contributions	53	101	37	77	41	67

[1] As given in Table 4 scaled by the factor $R/(R-1)$ (about 1.08). See Section 4.5.

[2] Contribution clue to the uncertainty in selecting the same reference point on the radiostructure for the maps from the two frequency bands. See Section 4.5.

[3] Based on the standard deviations of the parameter values given in footnote to Table 2.

[4] As given in Table 3. See Section 4.4.

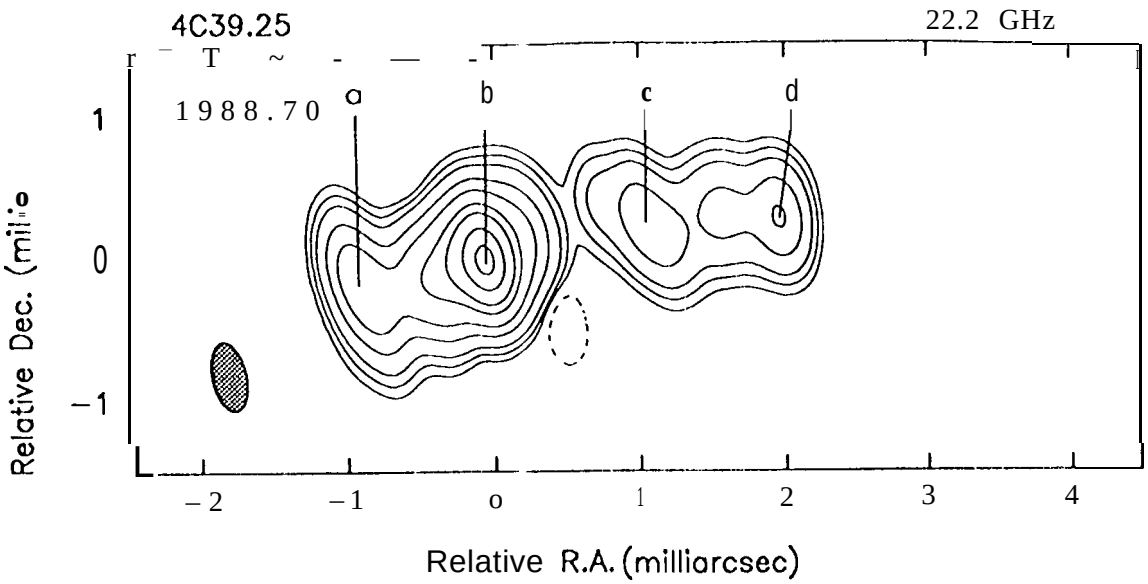
4C39.25
22.2 GHz
1988.70
a
b
c
d
1
0
−1
−2
−1
0
1
2
3
4
Relative Dec. (milli
Relative R.A. (milliarcsec)

Fig. 1

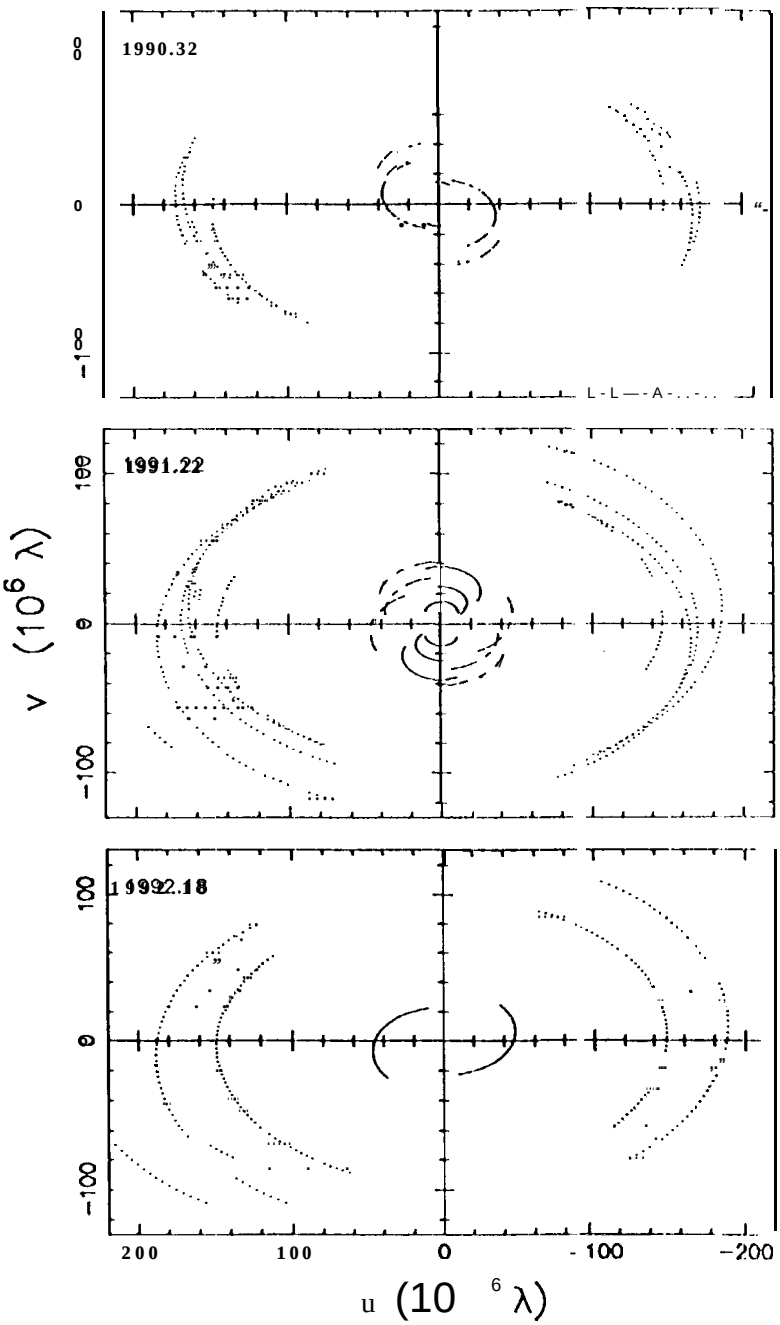

Fig. 2

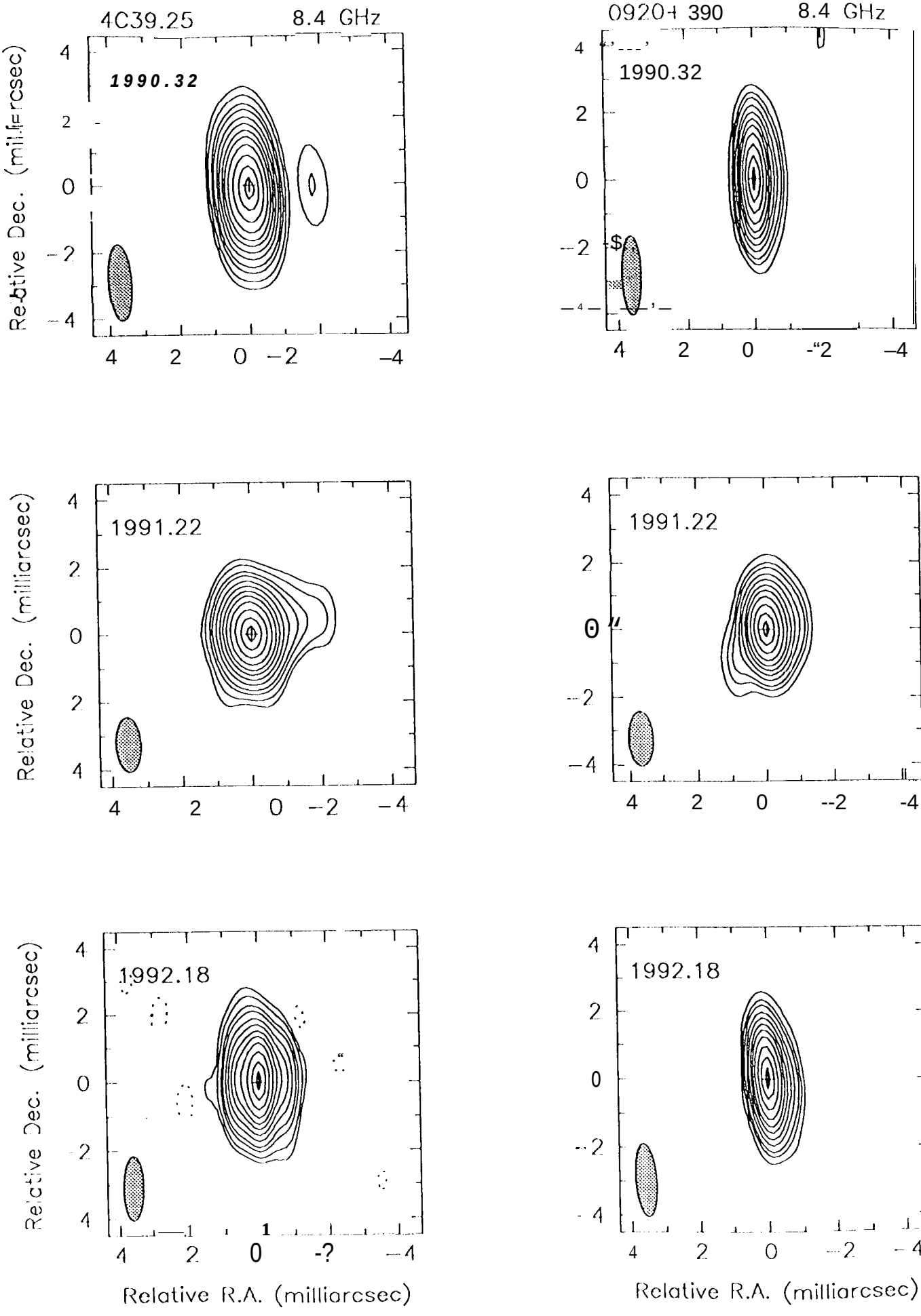
4C39.25
8.4 GHz
1990.32
0920+390
8.4 GHz
1990.32
1991.22
1991.22
1992.18
1992.18
Relative Dec. (milliarcsec)
Relative R.A. (milliarcsec)

Fig.

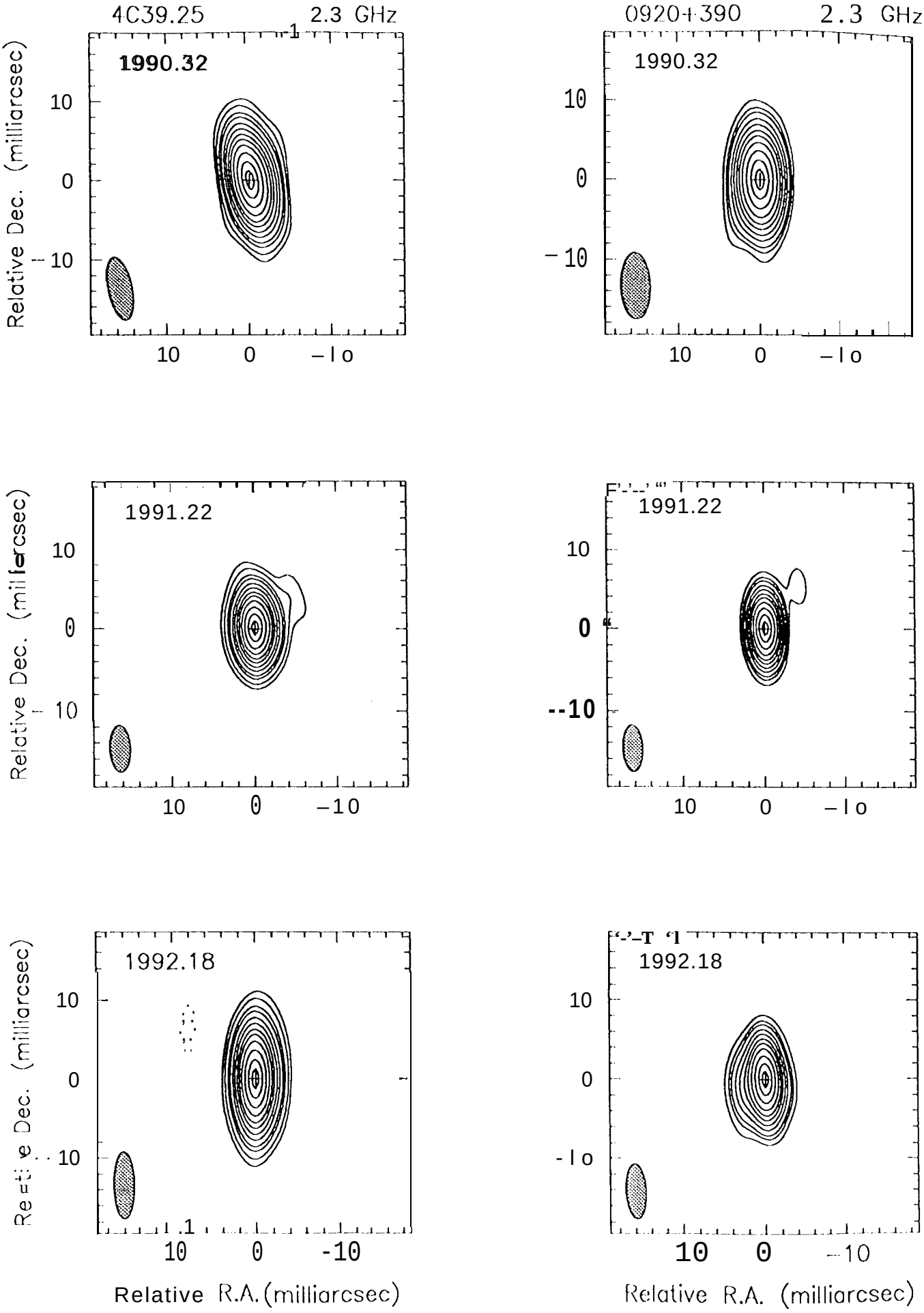
4C39.25
2.3 GHz
1990.32
0920+390
2.3 GHz
1990.32
1991.22
1991.22
1992.18
1992.18
Relative Dec. (milliarcsec)
Relative R.A. (milliarcsec)
Relative R.A. (milliarcsec)

Fig. 4

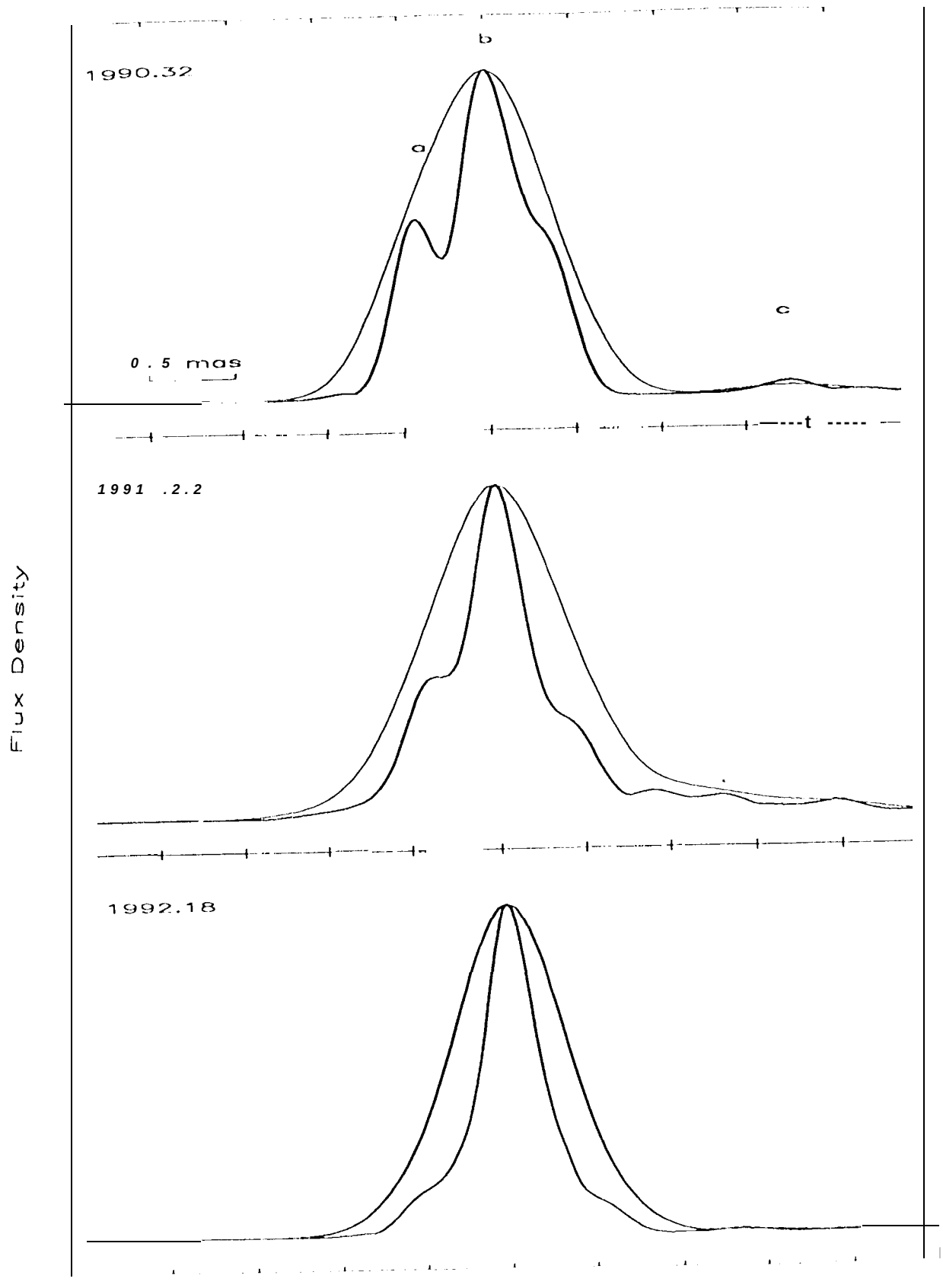
b
1990.32
a
c
0.5 mas
t
1991.2.2
1992.18
Flux Density
Distance along the jet

Fig.

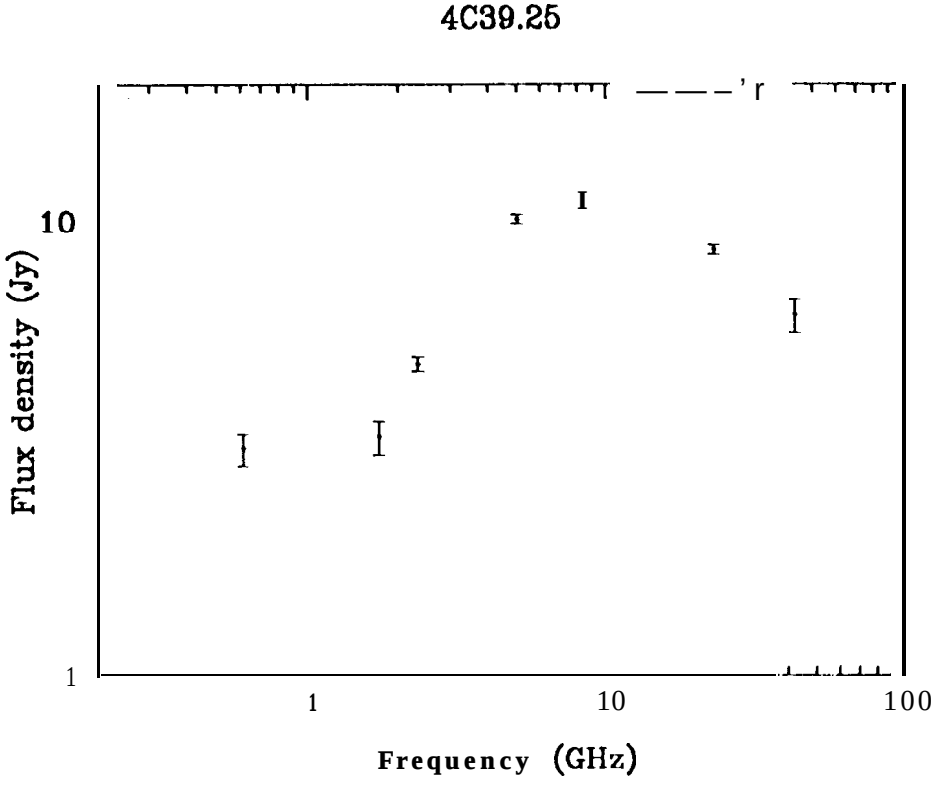

Fig. 6

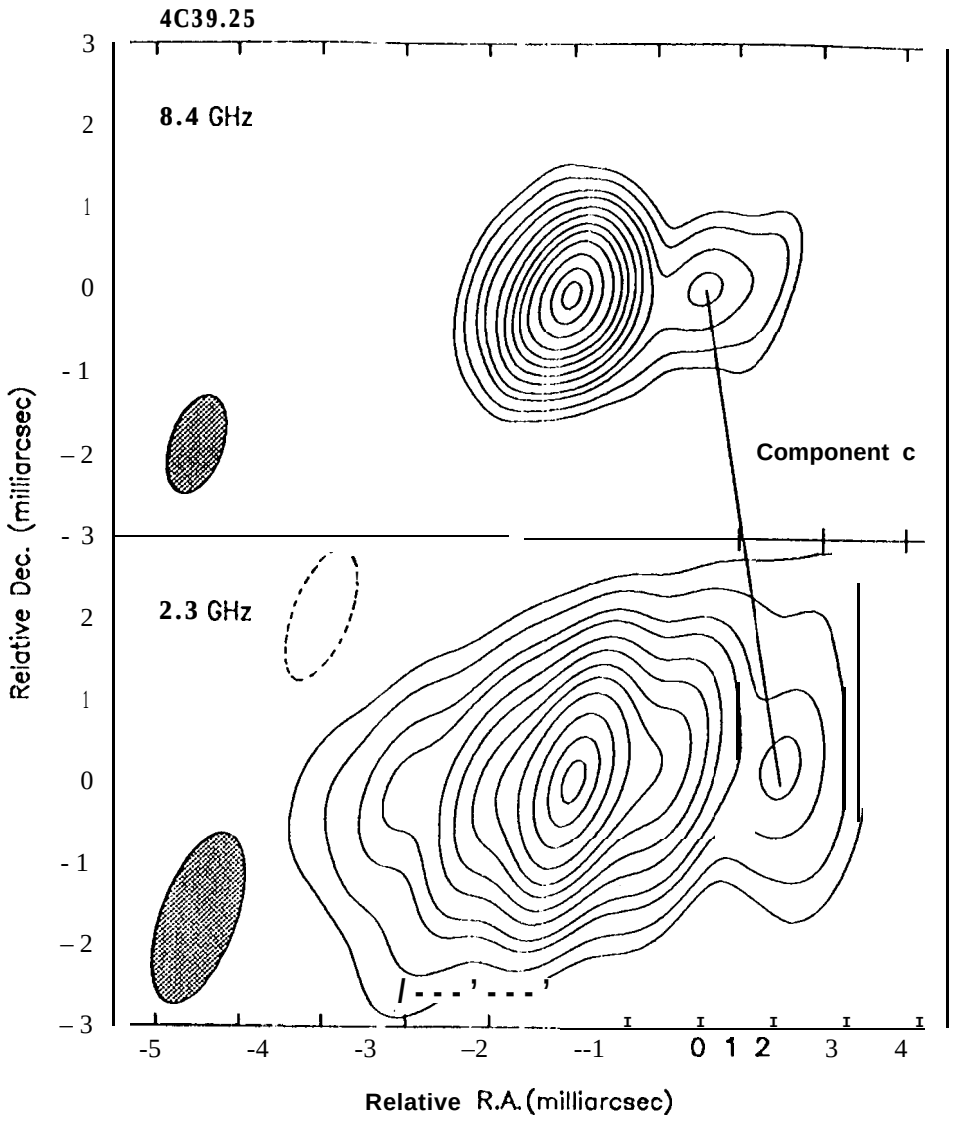
4C39.25
8.4 GHz
2.3 GHz
Component c
Relative Dec. (milliarcsec)
Relative R.A.(milliarcsec)
3
2
1
0
- 1
– 2
- 3
-5
-4
-3
–2
--1
0 1 2
3
4

Fig. 7

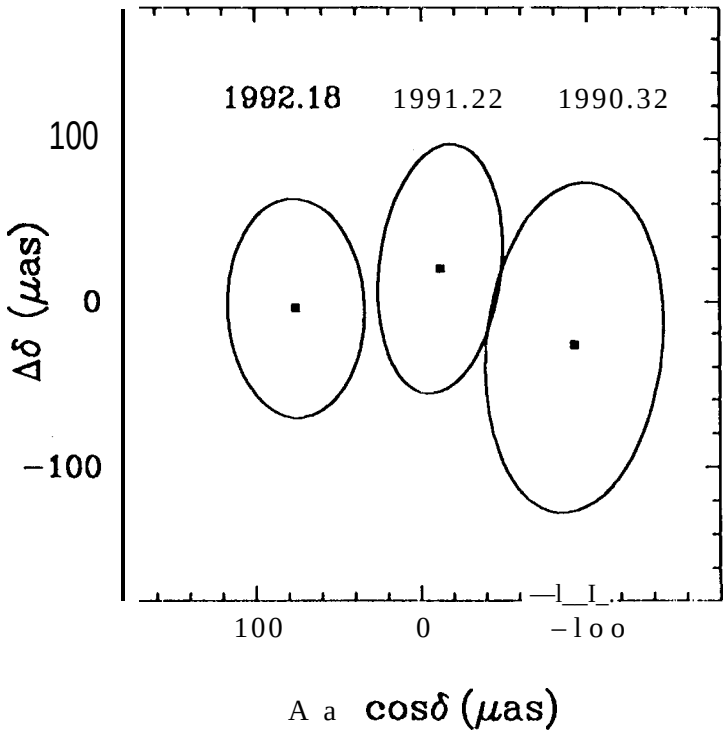

Fig. 8

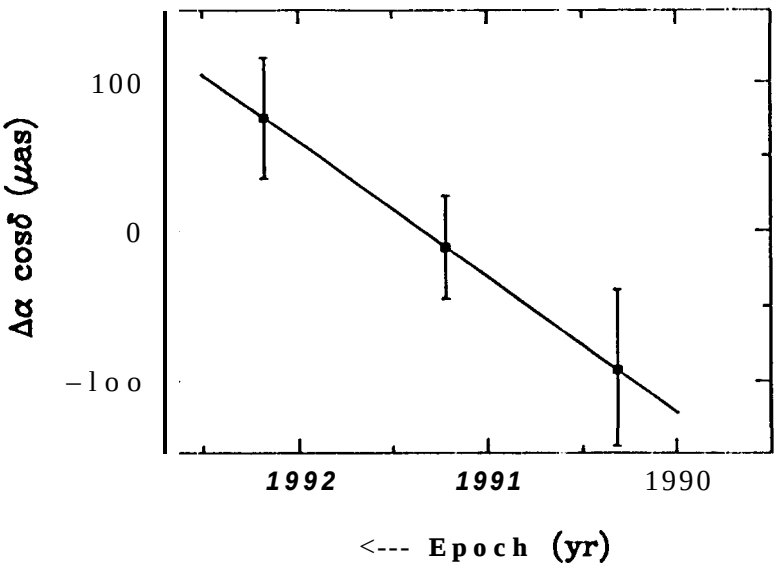
100
0
−loo
Δα cosδ (μas)
1992
1991
1990
<--- Epoch (yr)

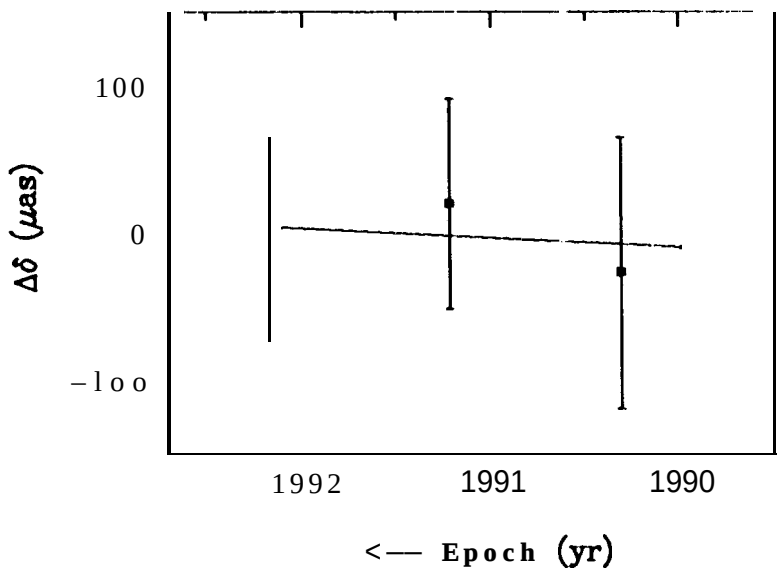
100
0
−loo
Δδ (μas)
1992
1991
1990
<— Epoch (yr)

Fig. 9